Int. J. Heat Mass Transfer. Vol. 29, No. 9, pp. 1371–1381, 1986
Printed in Great Britain

0017 9310/86 $3.00 + 0.00
Pergamon Journals Ltd.

Natural convection of gas/vapour mixtures in a porous medium

MALCOLM R. DAVIDSON

CSIRO Division of Mineral Engineering, Lucas Heights Research Laboratories, Private Mail Bag 7, Sutherland, NSW 2232, Australia

(*Received* 28 *May* 1985 *and in final form* 22 *January* 1986)

Abstract—A two-component model of the natural convection of gas/vapour mixtures is described in which the temperature dependence of mixture properties is incorporated. Attention is focused on a two-dimensional packed bed with isothermal top and bottom plates and insulated side walls; nitrogen/water vapour and helium/water vapour mixtures are considered. When the mixture density is a monotonic function of temperature and the temperature difference is small ($\approx 10°C$), predicted values of the critical Rayleigh number (Ra_c), modes of convection, flow and temperature distribution agreed well (1–2 percent in Ra_c) with corresponding values derived from an analogous single-component model based on properties evaluated at the mean temperature; the increasing difference between such values as the temperature difference increases is also shown.

INTRODUCTION

CLOSE [1] proposed a method for storing thermal energy in packed beds in which a fluid mixture with one condensing component is used. In a typical arrangement, vapour is generated by heating a liquid pool at the base of the container and the amount of non-condensing gas is adjusted to maintain the system at atmospheric pressure; heat is extracted at the top of the container. Transport of heat is enhanced by natural convection but the effect is much greater for a gas/vapour mixture in which the vapour is continually condensing and re-evaporating than it is for the gas alone. Close [1] demonstrated this by using an analogous single-component model for the gas/vapour mixture in which the property-dependent coefficients are evaluated at the mean temperature. However, although this concept has been confirmed by experimental data [2], no theoretical study of the flow mechanics operating or of the limitations of the model is available. Natural convection of gas and vapour may also occur in the underground heating of soils (e.g. as an aid to agriculture), or may be useful in the design of thermal diodes (conducting at night but insulating by day).

In this paper, a two-component model is developed which takes account of property variations of the mixture but which ignores mass diffusion of the gas and vapour components. To render the problem amenable to analysis, the model is extrapolated to near zero flow conditions and the "onset" criteria for convection, and the corresponding flow and temperature patterns, are then compared with those derived from the analogous single-component model for nitrogen/water vapour and helium/water vapour mixtures.

THE GOVERNING EQUATIONS

Cheng [3] derived the equations governing convective heat transfer in a porous medium saturated with a liquid and its vapour under assumptions of local thermodynamic equilibrium. A similar analysis can be applied, when the vapour is replaced by a mixture of vapour and a non-condensing gas, to obtain the following equations expressing conservation of mass and energy for steady flow:

$$\nabla\cdot(\rho_v\mathbf{u}) = -\nabla\cdot\mathbf{J}+F, \tag{1}$$

$$\nabla\cdot(\rho_d\mathbf{u}) = \nabla\cdot\mathbf{J}, \tag{2}$$

$$\nabla\cdot(\rho_l\mathbf{u}_l) = -F, \tag{3}$$

$$\nabla\cdot(\rho\mathbf{u}h+\rho_l\mathbf{u}_l h_l) = k\nabla^2 T-\nabla\cdot(h_v-h_d)\mathbf{J}, \tag{4}$$

where

$$\mathbf{J} = -\rho D\nabla(\rho_v/\rho) = \rho D\nabla(\rho_d/\rho). \tag{5}$$

Here ρ, h, u, P denote density, specific enthalpy, Darcy velocity and pressure of the gas/vapour mixture; when these variables appear with subscripts v, d or l, they then refer to the vapour, non-condensing gas and liquid, respectively. The temperature T is the same at a given point in the solid matrix, liquid phase and gas mixture. Like ρ, densities ρ_v and ρ_d are defined in terms of mass per unit volume of gas mixture so that

$$\rho = \rho_v+\rho_d \tag{6}$$

and

$$\rho h = \rho_v h_v+\rho_d h_d. \tag{7}$$

The source term F in equations (1) and (3) represents the mass flux of vapour/unit volume of the porous

NOMENCLATURE

c_p, c_{pv}, c_{pd}, c_{pl} specific heat of gas/vapour mixture, vapour, non-condensing gas and liquid, respectively
c^* effective specific heat in analogous single-component model
D diffusivity of gas/vapour mixture
f_1-f_4 functions defined by equation (26)
F mass flux of vapour generated locally per unit volume
g gravitational acceleration
G dimensionless parameter defined by equation (25)
h, h_v, h_d, h_l specific enthalpy of gas/vapour mixture, vapour, non-condensing gas and liquid, respectively
$h_{vl} = h_v - h_l$, latent heat of vaporisation of condensing component
H height of packed bed
$\mathbf{J}$ binary diffusion flux in gas/vapour mixture
k thermal conductivity of packed bed saturated with gas, vapour and liquid
K, K_l permeability of porous medium to gas/vapour mixture and liquid, respectively
L width of packed bed
m mass fraction (ρ_v/ρ_d) of condensing component in gas/vapour mixture relative to the non-condensing component
M molecular weight
n horizontal wave number
P, P_v, P_d, P_l pressure of gas/vapour mixture, vapour, non-condensing gas and liquid, respectively
ΔP capillary pressure $P-P_l$
R universal gas constant
Ra Rayleigh number [defined by equation (32)]
S liquid saturation
T absolute temperature
$\Delta T = T_b - T_u$
$\mathbf{u}$, $\mathbf{u}_l$ velocity of gas/vapour mixture and liquid, respectively
(u, w), (u_l, w_l) components of $\mathbf{u}$ and $\mathbf{u}_l$, respectively
$W_l = \mu\rho_l w_l'/K\bar{\rho}^2 g$, dimensionless vertical liquid velocity
(x, z) coordinates as in Fig. 1
(X, Z) dimensionless coordinates $(x, z)/H$
$\hat{\mathbf{z}}$ unit vector in positive z direction.

Greek symbols
$\alpha_n = n\pi H/L$
θ dimensionless temperature perturbation $T'/\Delta T$
μ, μ_l viscosity of gas/vapour mixture and liquid, respectively
ρ, ρ_v, ρ_d, ρ_l density of gas/vapour mixture, vapour, non-condensing gas and liquid, respectively
$\bar{\rho}$ reference mixture density
Ψ dimensionless stream function $\mu\Psi'/KHg\bar{\rho}^2$.

Subscripts
v vapour
l liquid
d non-condensing gas
o unperturbed (basic) state
b bottom plate
u top plate
c critical
n mode of eigenvalue or eigenvector.

Superscript
$'$ perturbation from basic state.

medium crossing microscopic liquid–vapour interfaces during condensation or evaporation, $\mathbf{J}$ is the binary diffusion flux in the gas/vapour mixture for which D denotes the diffusivity, and k is the effective thermal conductivity (assumed constant) of the porous medium saturated with liquid and the gas/vapour mixture. In the thermal energy equation (4), viscous dissipation and pressure variation effects have been ignored (these are usually important only at very high flow velocities (see, e.g. Knudsen and Katz [4]), and the additional last term represents the heat transfer due to interdiffusion of the gas and vapour.

The flow of the gas/vapour mixture is assumed to satisfy Darcy's Law

$$\mathbf{u} = -\frac{K}{\mu}(\nabla P + \rho g\hat{\mathbf{z}}), \tag{8}$$

where μ denotes viscosity, g is the acceleration due to gravity, $\hat{\mathbf{z}}$ is a unit vector directed vertically upwards and K is the permeability of the porous medium. Similarly, Darcy's Law for the liquid flow is

$$\mathbf{u}_l = -\frac{K_l}{\mu_l}(\nabla P_l + \rho_l g\hat{\mathbf{z}}), \tag{9a}$$

where P_l differs from P owing to interfacial tension effects. Both the effective permeability K_l and the capillary pressure $\Delta P = P - P_l$ depend empirically on the local liquid saturation (S) in the porous medium. Following Close [1], the gas flow properties of the porous medium are assumed to be unaffected by the flow of liquid. Thus K in equation (8) takes its saturated value and the liquid is assumed to occupy only a small fraction of the void space. [Close (personal

communication) has observed the liquid occurring as a thin layer coating the packing material when the gas consists of air and water vapour or air and the ethyl alcohol azeotrope.] Capillary and gravitational effects are expected to be the important factors driving the flow of liquid, with gas pressure gradients having little influence. Furthermore, we ignore horizontal variations in liquid saturation and, like Close, assume that the liquid only flows vertically. Thus we replace equation (9a) by

$$\mathbf{u}_l = w_l \hat{\mathbf{z}}, \tag{9b}$$

where the unknown w_l is to be determined without specifying the functions $\Delta P(S)$ and $K_l(S)$. However, it is not strictly necessary to assume a vertical liquid velocity since an analysis which incorporates equation (9a) can be developed; of course the functions $\Delta P(S)$ and $K_l(S)$ must then be given.

The mass balance equations (1–3), together with relations (6) and (7), reduce the energy equation (4) to

$$\rho_v \mathbf{u}\cdot\nabla h_v + \rho_d \mathbf{u}\cdot\nabla h_d + \rho_l \mathbf{u}_l\cdot\nabla h_l = k\nabla^2 T - (h_v - h_l)\nabla\cdot(\rho\mathbf{u}) - \mathbf{J}\cdot\nabla(h_v - h_d). \tag{10}$$

Since we are ignoring pressure variations in the energy equation the specific enthalpies h_v, h_d and h_l are assumed to depend linearly on temperature with slopes (specific heats) c_{pv}, c_{pd} and c_{pl}, respectively. This is usually a good approximation (e.g. Knudsen and Katz [4], p. 9), but for ideal gases the linear dependence is exact. The energy equation then becomes

$$\rho c_p \mathbf{u}\cdot\nabla T + \rho_l c_{pl}\mathbf{u}_l\cdot\nabla T = k\nabla^2 T - h_{vl}\nabla\cdot(\rho u) - (c_{pv} - c_{pd})\mathbf{J}\cdot\nabla T, \tag{11}$$

where c_p, the specific heat of the gas mixture, is defined by

$$\rho c_p = \rho_v c_{pv} + \rho_d c_{pd} \tag{12}$$

and

$$h_{vl} = h_v - h_l \tag{13}$$

is the latent heat of vaporisation, the quantities ρ, c_p and h_{vl} depending on temperature. The last term in equation (11), associated with the enthalpy transfer by gas-vapour interdiffusion, appears in the literature of laminar film condensation (e.g. Minkowycz and Sparrow [5]); the second last term, representing the enthalpy transfer due to vapour formation, occurs analogously in a study of two-phase convection [Schubert and Straus [6]; first term of their equation (18)].

Following Close [1], we now assume that the gas and the vapour behave as ideal gases; thus

$$P_v = \rho_v RT/M_v, \quad P_d = P - P_v = \rho_d RT/M_d, \tag{14}$$

with T measured in degrees absolute, and we have Close's equations (13) and (14):

$$\rho = \frac{P(1+m)M_v M_d}{RT(M_v + mM_d)} \tag{15}$$

and

$$m = \frac{M_v P_v}{M_d(P - P_v)}, \tag{16}$$

where $m = \rho_v/\rho_d$. Continuing, we suppose that the vapour and the liquid at any point are in equilibrium, the partial pressure P_v of the vapour being related to temperature by the Clausius–Clapeyron equation

$$\frac{dP_v}{dT} = \frac{M_v P_v h_{vl}}{RT^2}. \tag{17}$$

Like Close, we assume that the properties of the gas/vapour mixture are independent of the pressure variations within it; thus ρ_v, ρ_d (and hence ρ, m) are regarded as functions of T alone with a constant value (1 atmosphere) assigned to the pressure P.

If we now take the liquid to be incompressible, and use the above property/temperature relationships then, in principle, equations (1–3), (5), (8), (9b) and (11), together with appropriate boundary conditions, are sufficient to determine the system. However, it is convenient to make a further simplification: diffusion is assumed to contribute little to the mass flux of the non-condensing gas or the vapour, therefore we neglect $\mathbf{J}$ relative to $\rho_d\mathbf{u}$ and $\rho_v\mathbf{u}$ in which case $\mathbf{J}$ disappears not only from the mass balance equations (1) and (2) but also from the reduced energy equation (10). In an air/water vapour mixture, for example, diffusion velocities ($\mathbf{J}/\rho_d$, $\mathbf{J}/\rho_v$) typically range in value up to about 5 cm/h (based on $D = 0.04$ cm^2/s and $|\nabla T| = 50$°C/m) which we regard as small. Only when the temperature is very close to the boiling point does the air diffusion velocity begin to increase rapidly (e.g. 30–60 cm/h when $T = 98$–99°C).

Collecting the governing equations together into a simplified set based on our assumptions, we have

$$\nabla\cdot(\rho\mathbf{u} + \rho_l w_l\hat{\mathbf{z}}) = 0 \quad \text{[adding equations (1–3)]}, \tag{18a}$$

$$\nabla\cdot(\rho_d\mathbf{u}) = 0, \tag{18b}$$

$$\rho c_p \mathbf{u}\cdot\nabla T + \rho_l c_{pl} w_l \hat{\mathbf{z}}\cdot\nabla T = k\nabla^2 T - h_{vl}\nabla\cdot(\rho\mathbf{u}), \tag{18c}$$

and

$$\mathbf{u} = -\frac{K}{\mu}(\nabla P + \rho g\hat{\mathbf{z}}) \quad \text{[equation (8)]} \tag{18d}$$

to solve for the unknowns $\mathbf{u}$, w_l, T and P.

We now restrict our attention to two-dimensional flow in a container with rectangular cross-section (height H, width L) and use rectangular coordinates (x, z) as shown in Fig. 1. The top and bottom plates are maintained at constant temperatures T_u and T_b, respectively, and the side walls are insulated. The vertical mass flux of the gas/vapour mixture is zero at the top and bottom; that of the liquid is zero at the top but, in general, is non-zero locally (in a manner to be determined) at the liquid pool at the base, although the average mass flux there must be zero. The bound-

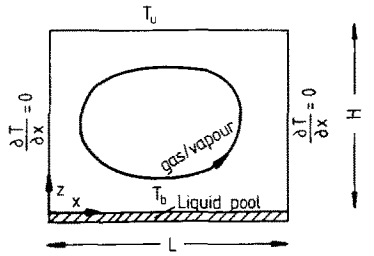

FIG. 1. Schematic representation of the two-dimensional packed bed.

ary conditions are therefore

$$T = T_u,\ w = w_l = 0 \text{ on } z = H,$$

$$T = T_b,\ w = 0 \text{ on } z = 0, \text{ and}$$

$$\partial T/\partial x = u = 0 \text{ on } x = 0 \text{ and } x = L,$$

where u and w denote the components of $\mathbf{u}$ in the x and z directions, respectively.

To render the solution of equations (18a–d) amenable to analysis, we now extrapolate to near zero flow and investigate the "onset" of convection in the container using a linear stability analysis by considering small perturbations from the simple conduction solution [$\mathbf{u} = w_l = 0$, and $T = T_b - (T_b - T_u)z/H$].

Of course, a proper analysis at very low flows must include mass diffusion effects, since diffusive and convective fluxes are then of similar order, in which case there is not even a stagnant state since small liquid and gas flows must occur to balance the mass diffusion. However, it is our intention to compare the extrapolated perturbation solution with that corresponding to the equivalent single-component model. In both cases, mass diffusion is ignored (Close [1, 2] retains such a term in the energy equation but a good fit with the data can be achieved without it), so its absence should not affect a discussion which compares the two models. Furthermore, the flow mechanisms highlighted by the analysis of this paper should be the same as those acting at much larger velocities; only the details will be different. Finally, the perturbation solution is the first term of an expansion (based on the method of Palm *et al.* [7]) which is valid for finite amplitude flows for which ignoring mass diffusion is a much better approximation.

THE LINEARISED PROBLEM

We now follow the usual procedure for a stability analysis and set

$$T = T_o + T', \quad (u, w) = (u', w'), \quad w_l = w_l',$$

$$P = P_o + P', \qquad \rho = \rho_o + \rho',$$

where the primed variables are small perturbations from the pure conduction solution which, in turn, is signified by the subscript 'o'. When these forms are substituted into equations (18a–d), with density perturbations approximated to first order [$\rho' = (\mathrm{d}\rho_o/\mathrm{d}T)T'$] and the products of perturbations ignored, we obtain

$$\nabla\cdot(\rho_o\mathbf{u}' + \rho_l w_l'\hat{\mathbf{z}}) = 0, \tag{19a}$$

$$\nabla\cdot(\rho_{do}\mathbf{u}') = 0, \tag{19b}$$

$$(\rho_o c_p(T_o)w' + \rho_l c_{pl} w_l')\frac{\mathrm{d}T_o}{\mathrm{d}z} = k\nabla^2 T' - h_{vl}(T_o)\nabla\cdot(\rho_o\mathbf{u}'), \tag{19c}$$

and

$$\mathbf{u}' = -\frac{K}{\mu}\left(\nabla P' + \frac{\mathrm{d}\rho_o}{\mathrm{d}T}T'g\hat{\mathbf{z}}\right), \tag{19d}$$

where ρ_o and ρ_{do} are functions of T_o and hence z, independent of x. Eliminating P' from equation (19d) gives

$$\frac{\partial u'}{\partial z} - \frac{\partial w'}{\partial x} = \frac{K}{\mu}\frac{\mathrm{d}\rho_o}{\mathrm{d}T}g\frac{\partial T'}{\partial x}, \tag{20}$$

and using equation (19b) together with the relation

$$\rho_o = \rho_{do}(1 + m_o),$$

we can show that

$$\nabla\cdot(\rho_o u') = \rho_{do} w'\frac{\mathrm{d}T_o}{\mathrm{d}z}\frac{\mathrm{d}m_o}{\mathrm{d}T}. \tag{21}$$

Equation (19b) is satisfied by defining a stream function Ψ' where

$$\rho_{do}u' = \frac{\partial\Psi'}{\partial z}, \quad \rho_{do}w' = -\frac{\partial\Psi'}{\partial x}. \tag{22}$$

Equations (20–22) reduce (19a–d) to

$$\left(\rho_l c_{pl} w_l' - (1 + m_o)c_p(T_o)\frac{\partial\Psi'}{\partial x}\right)\frac{\mathrm{d}T_o}{\mathrm{d}z} = k\left(\frac{\partial^2 T'}{\partial x^2} + \frac{\partial^2 T'}{\partial z^2}\right) + h_{vl}(T_o)\frac{\mathrm{d}m_o}{\mathrm{d}T}\frac{\mathrm{d}T_o}{\mathrm{d}z}\frac{\partial\Psi'}{\partial x}, \tag{23a}$$

$$\rho_l\frac{\partial w_l'}{\partial z} = \frac{\mathrm{d}m_o}{\mathrm{d}T}\frac{\mathrm{d}T_o}{\mathrm{d}z}\frac{\partial\Psi'}{\partial x}, \tag{23b}$$

$$\frac{\partial^2\Psi'}{\partial x^2} + \frac{\partial^2\Psi'}{\partial z^2} - \frac{1}{\rho_{do}}\frac{\mathrm{d}\rho_{do}}{\mathrm{d}T}\frac{\mathrm{d}T_o}{\mathrm{d}z}\frac{\partial\Psi'}{\partial z} = \frac{K}{\mu}\rho_{do}\frac{\mathrm{d}\rho_o}{\mathrm{d}T}g\frac{\partial T'}{\partial x}. \tag{23c}$$

It is convenient to make equations (23a–c) non-dimensional by setting

$$(X, Z) = (x, z)/H, \qquad \theta = T'/\Delta T,$$

$$\Psi = \mu\Psi'/KHg\bar{\rho}^2, \quad W_l = \mu\rho_l w_l'/K\bar{\rho}^2 g,$$

where $\bar{\rho}$ is a reference mixture density and $\Delta T = T_b - T_u$. After noting, in addition, that $\mathrm{d}T_o/\mathrm{d}z =$

$-\Delta T/H$, equations (23a–c) become

$$\frac{\partial^2\theta}{\partial X^2}+\frac{\partial^2\theta}{\partial Z^2}=G\left[f_1(Z)\frac{\partial\Psi}{\partial X}-W_1\right], \quad (24a)$$

$$\frac{\partial W_1}{\partial Z}=-f_2(Z)\frac{\partial\Psi}{\partial X}, \quad (24b)$$

and

$$\frac{\partial^2\Psi}{\partial X^2}+\frac{\partial^2\Psi}{\partial Z^2}+f_3(Z)\frac{\partial\Psi}{\partial Z}=f_4(Z)\frac{\partial\theta}{\partial X}, \quad (24c)$$

where

$$G=\frac{c_{pl}Hg\bar{\rho}^2K}{k\mu}, \quad (25)$$

$$f_1(Z)=\left[(1+m_o)c_p(T_o)+h_{vl}(T_o)\frac{dm_o}{dT}\right]\Big/c_{pl}, \quad (26a)$$

$$f_2(Z)=\frac{dm_o}{dT}\Delta T, \quad (26b)$$

$$f_3(Z)=\frac{1}{\rho_{do}}\frac{d\rho_{do}}{dT}\Delta T, \quad (26c)$$

and

$$f_4(Z)=\rho_{do}\frac{d\rho_o}{dT}\Delta T/\bar{\rho}^2. \quad (26d)$$

The boundary conditions, in terms of the dimensionless variables, are

$$\theta=\Psi=W_1=0 \text{ on } Z=1,$$

$$\theta=\Psi=0 \text{ on } Z=0,$$

$$\frac{\partial W_1}{\partial X}=\frac{\partial\theta}{\partial X}=\Psi=0 \text{ on } X=0 \text{ and } X=L/H.$$

Thus θ, Ψ and W_1 may be expressed as

$$\theta=\sum_{n=1}^{\infty}\theta_n(Z)\cos\alpha_nX, \quad (27a)$$

$$\Psi=\sum_{n=1}^{\infty}\Psi_n(Z)\sin\alpha_nX, \quad (27b)$$

and

$$W_1=\sum_{n=1}^{\infty}W_{1n}(Z)\cos\alpha_nX, \quad (27c)$$

where $\alpha_n=n\pi H/L$. Substituting equations (27a–c) into (24a–c) yields the following system of ordinary differential equations for θ_n, Ψ_n and W_{1n}:

$$\ddot{\theta}_n-\alpha_n^2\theta_n=G(\alpha_nf_1\Psi_n-W_{1n}) \quad (28a)$$

$$\dot{W}_{in}=-\alpha_nf_2\Psi_n \quad (28b)$$

$$\ddot{\Psi}_n+f_3\dot{\Psi}_n-\alpha_n^2\Psi_n=-\alpha_nf_4\theta_n, \quad (28c)$$

where "˙" denotes differentiation with respect to Z. Together with the boundary conditions,

$$\theta_n(0)=\theta_n(1)=0,$$

$$\Psi_n(0)=\Psi_n(1)=0,$$

$$W_{1n}(1)=0,$$

equations (28a–c) constitute an eigenvalue problem for G, given the ratio L/H, top and bottom temperatures T_u and T_b, and the horizontal wave number n. The value of n which achieves the smallest (critical) value of G defines the predicted onset mode of convection.

The above eigenvalue problem can be solved routinely by numerical methods. The derivatives in equations (28a–c) are approximated by central finite differences and the resulting system of linear algebraic equations solved for the smallest positive eigenvalue G together with its eigenvectors. In equations (28b), $\dot{W}_{1n}$ is approximated by using adjacent mesh points, with the right side of the equation being evaluated at the mid point to ensure a conservative form.

THE EFFECTIVE SINGLE-COMPONENT MODEL

To transform the energy equation into a form analogous to that for convection of a single gas, Close [1] effectively neglects the second term of equation (18c). Equation (18c) then reduces to

$$\rho_dc^*\mathbf{u}\cdot\nabla T=k\nabla^2T, \quad (29)$$

since

$$\nabla\cdot(\rho\mathbf{u})=\nabla\cdot(\rho_v\mathbf{u})=\nabla\cdot(m\rho_d\mathbf{u})=\rho_d\mathbf{u}\cdot\nabla m$$

[using equation (18b)]. Here

$$c^*=(1+m)c_p+h_{vl}dm/dT \quad (30)$$

is the effective specific heat. The coefficients of equation (29) are the same as those of Close's corresponding equation (9) except that mass diffusion has been omitted.

Equations (18b), (18d) and (29) describe the effective single-component model with constant values being taken for ρ_d, c^* and $d\rho/dT$ (corresponding to standard assumptions for natural convection of a single fluid, see, e.g. Combarnous and Bories [8]). A dimensional analysis then yields the familiar Rayleigh number.

$$Ra=\frac{g(-d\rho/dT)(\rho_dc^*)K\Delta TH}{\mu k} \quad (31)$$

and the known results for this problem can be applied. Of course Ra is really temperature-dependent and in this paper we determine critical values of Ra (evaluated at the unperturbed state and denoted by Ra_c) as functions of vertical position z from critical G values (derived according to Section 3) where, from equations (25) and (31),

$$Ra=-\frac{G\Delta T}{c_{pl}\bar{\rho}^2}\rho_dc^*\frac{d\rho}{dT}; \quad (32)$$

these are then compared with the critical Rayleigh number based on constant properties ($4\pi^2$, when $L/H=1$, see, e.g. Combarnous and Bories [8]). The

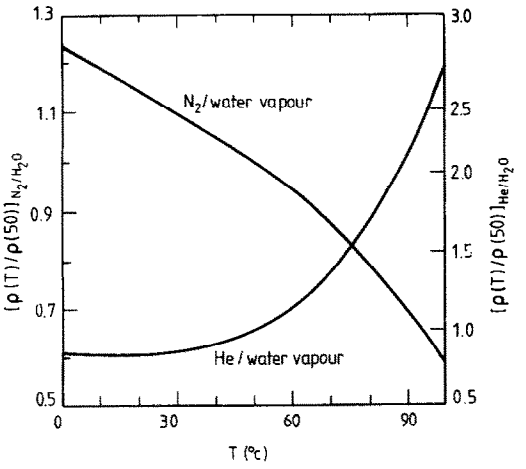

FIG. 2. Density variation with temperature of nitrogen/water vapour and helium/water vapour mixtures.

corresponding flow and temperature patterns are also compared.

COMPARISON OF TWO-COMPONENT AND SINGLE-COMPONENT MODELS

Most of the results which follow are based on an aspect ratio $L/H = 1$. Specific heat data presented in ref. [9] are used and calculated enthalpies and pressures for water vapour are checked against tabulated values (see e.g. Wark [10]).

We now consider N_2/water vapour and He/water vapour mixtures in turn. The mixture densities $\rho(T)$ for each case are shown in Fig. 2. Note that, although ρ_d and ρ_v respectively decrease and increase with increasing T, ρ decreases monotonically in the N_2 case but falls to a minimum at $T \approx 14°C$ before increasing in the He case. The minimum in the density variation (corresponding to the neutral buoyancy temperature described in Ref. [1]) of the He/water vapour mixture occurs because the molecular weight of He is lower than that of H_2O and, with increasing temperature, the mass fraction of the heavier component (H_2O) increases.

In Fig. 3, the variation in Ra_c with height z for N_2/water vapour in the two-component (TC) model is shown together with the Ra_c value ($4\pi^2$) arising from the single-component (SC) model based on the mean temperature properties (at $z/H = 0.5$). As was hoped, the value of Ra_c predicted by the TC model at the mean temperature approaches $4\pi^2$ as T_u approaches T_b. When $T_b = 90°C$ and $T_u = 80°C$, the percentage difference in these Ra_c values is about 2%; however, note the importance of basing the constant property SC model specifically on the mean temperature.

Figures 4 and 5 show contours of the stream function, temperature perturbation and liquid velocity for an N_2/water vapour mixture and compares results for the SC and TC models. The temperature perturbation is positive or negative as the gas/vapour mixture flows up (heat is convected from the hot surface $z = 0$) or down, respectively. Under stagnant conditions, gravity balances the upwards capillary suction but, when the gas/vapour mixture flows upwards, condensation of vapour increases the liquid fraction and so reduces capillary suction; the liquid then flows down. The opposite occurs when the gas/vapour mixture flows downwards.

For the smaller ΔT value ($T_b = 90°C$, $T_u = 80°C$), the stream functions shown in Fig. 4(a) for the SC and TC models are almost indistinguishable, whereas the corresponding differences in the temperature perturbation [Fig. 4(b)], resulting from the absence of the second term of equation (18c) from the SC model, are more pronounced. As was expected, all differences become exaggerated for the larger ΔT value in Figs. 5(a, b) ($T_b = 90°C$, $T_u = 20°C$). Whereas the temperature perturbation for the SC model exhibits a vertically symmetric pattern, that for the TC model is skewed towards the base. This can most easily be seen in terms of the SC model with temperature-dependent coefficients. From equation (29), the vertical convective heat flux is $\rho_d c^* w T$ which, from equation (22), is $-c^* T \partial \Psi'/\partial x$. If we now ignore SC–TC differences

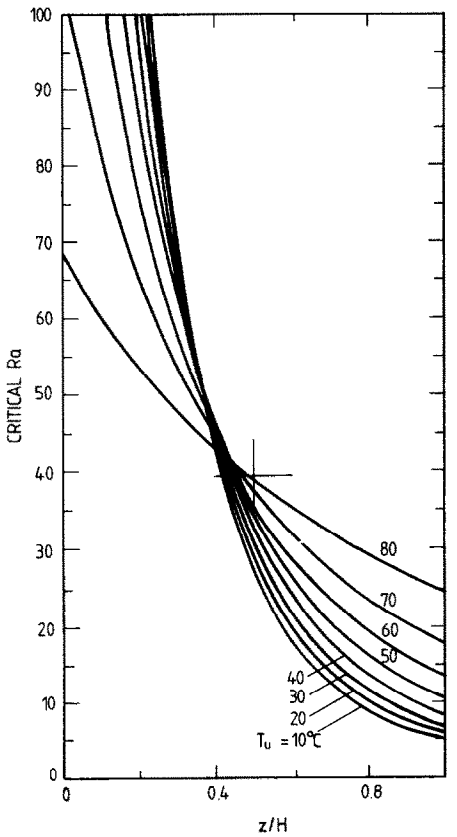

FIG. 3. Critical Rayleigh number for nitrogen/water vapour derived from the two-component model as a function of height (z) when $T_b = 90°C$ and $L/H = 1$ for various T_u values. The cross marks the critical value ($4\pi^2$) derived from a single-component model in which mixture properties are evaluated at the mean temperature.

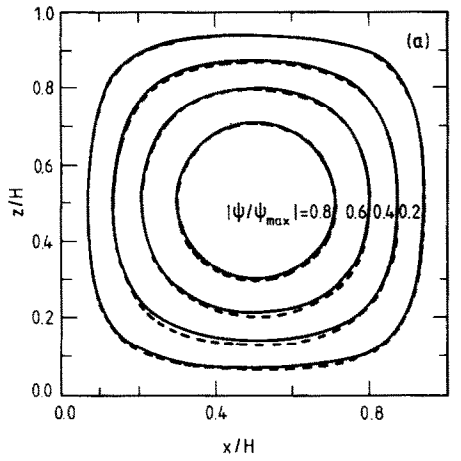

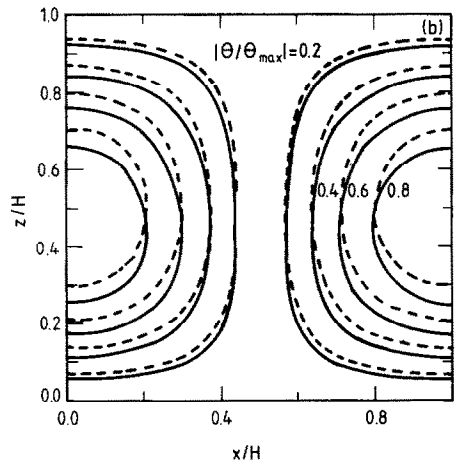

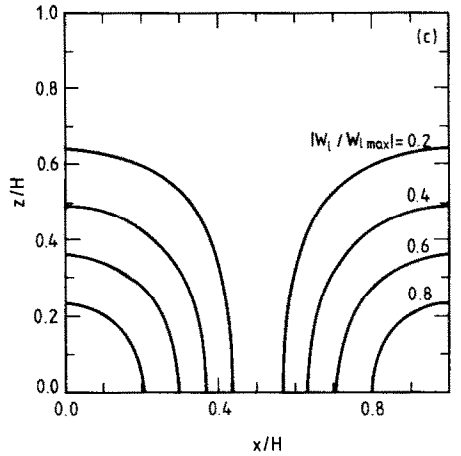

FIG. 4. (a) Stream function, (b) temperature perturbation, (c) (vertical) liquid velocity for onset mode of a nitrogen/water vapour mixture when $T_b = 90°C$, $T_u = 80°C$ and $L/H = 1$. Solid lines correspond to the two-component model and dashed lines to the analogous single-component model. In (b) and (c), contour values on the left and right are of opposite sign.

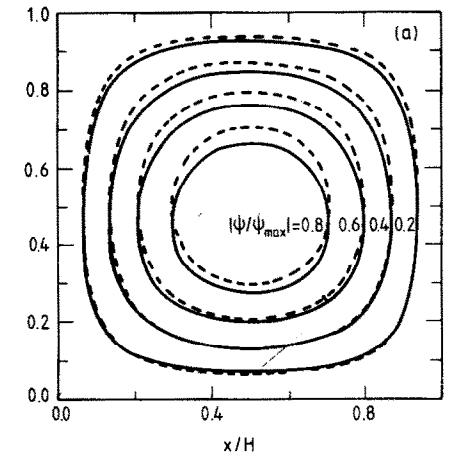

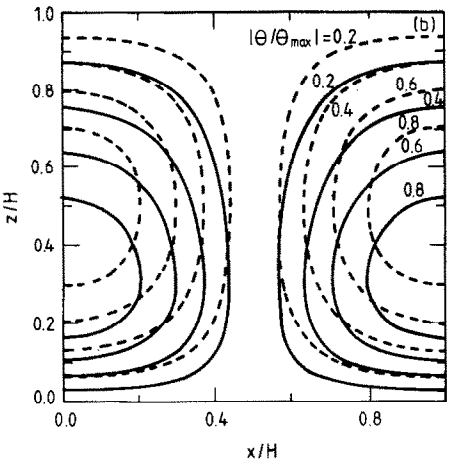

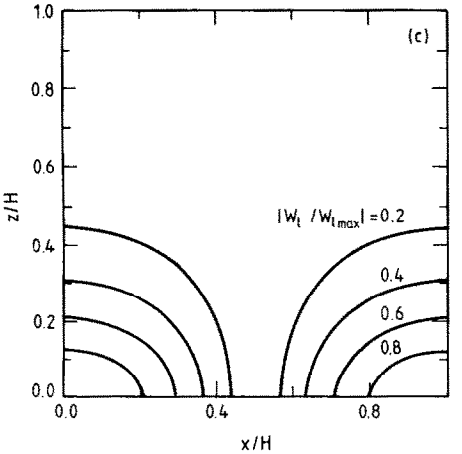

FIG. 5. (a) Stream function, (b) temperature perturbation, (c) (vertical) liquid velocity for onset mode of a nitrogen/water vapour mixture when $T_b = 90°C$, $T_u = 20°C$ and $L/H = 1$. Solid lines correspond to the two-component model and dashed lines to the analogous single-component model. In (b) and (c), contour values on the left and right are of opposite sign.

in $\partial\Psi'/\partial x$ and observe that c^* [defined by equation (30)] is greater at the bottom than at the top then, compared with the constant coefficient SC model, low values of T are effectively convected more rapidly to the bottom and high values less rapidly to the top; this accounts for the larger temperature perturbation at the bottom which, in turn, accounts for the reduced vertical extent of the circulation in Fig. 5(a).

A comparison of Figs. 4(c) and 5(c) shows that, for given T_b, the (vertical) liquid velocity decreases as T_u decreases. In that case, a given temperature, and hence the corresponding condensation of vapour, occurs lower in the container. However, at lower z values the difference between the gravitational force and capillary suction is less; liquid velocities are therefore smaller.

For the He/water vapour mixture, ρ increases with T for $T > 14°C$ and in this region circumstances are reversed. For convection to occur, the hot plate must now be at the top; the temperature perturbation is then negative or positive and the liquid rises or falls as the gas/vapour mixture rises or falls. However, it may be necessary to superimpose on the liquid flows described above a small downward flow (perhaps originating from a liquid-saturated sponge or injection spray at the top plate), otherwise the surface of the packing material can dry out under these (inverted) conditions (Close; personal communication). From Fig. 6, Ra_c predicted by the TC model

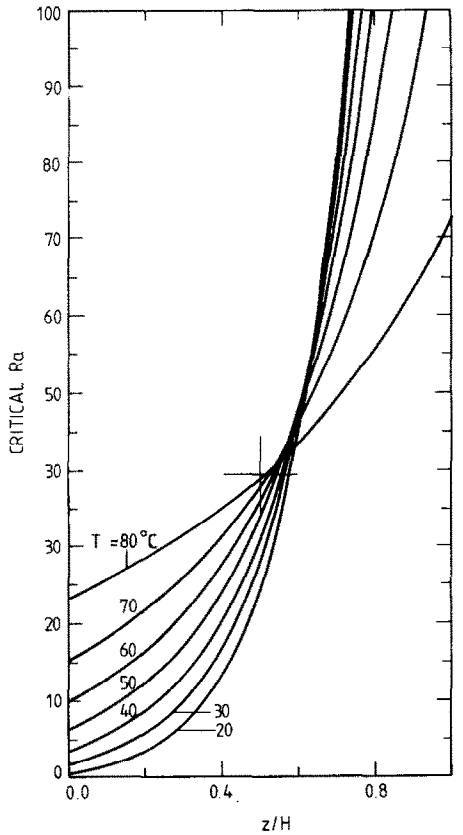

FIG. 6. Critical Rayleigh number for helium/water vapour derived from the two-component model as a function of height (z) when $T_u = 90°C$ and $L/H = 1$ for various T_b values. The cross marks the critical value ($4\pi^2$) derived from a single-component model in which mixture properties are evaluated at the mean temperature.

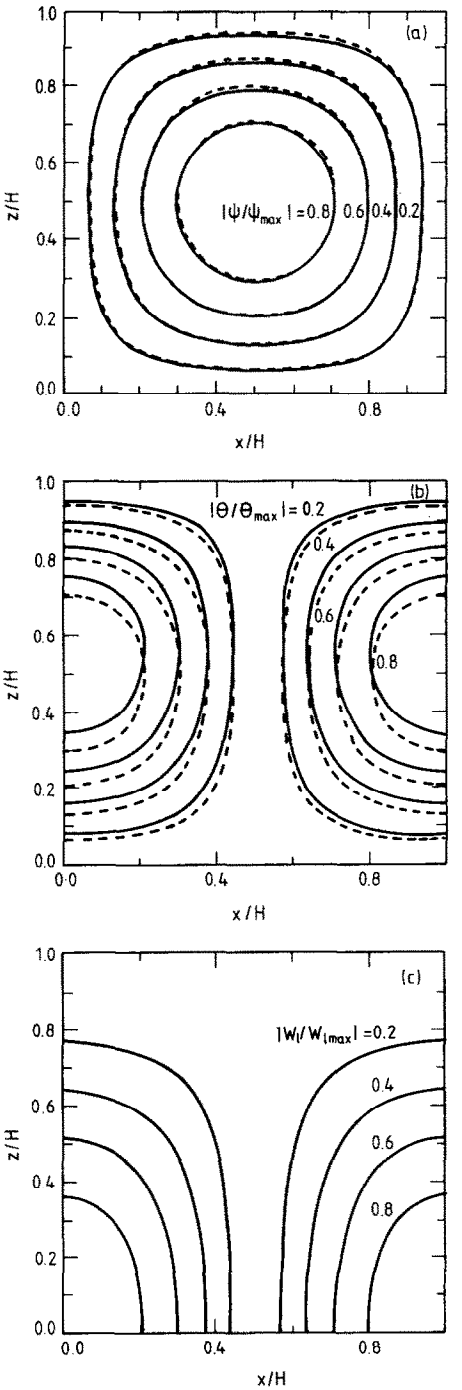

FIG. 7. (a) Stream function, (b) temperature perturbation, (c) (vertical) liquid velocity for onset mode of a helium/water vapour mixture when $T_u = 90°C$, $T_b = 80°C$ and $L/H = 1$. Solid lines correspond to the two-component model and dashed lines to the analogous single-component model. In (b) and (c), contour values on the left and right are of opposite sign.

at the mean temperature again approaches the SC value of $4\pi^2$ as ΔT decreases, the difference when $T_u = 90°C$ and $T_b = 80°C$ being about 1%. In that case, the SC and TC stream functions [Fig. 7(a)] are again almost identical, with the corresponding difference in the temperature perturbation [Fig. 7(b)] being more pronounced. The temperature perturbation in Fig. 8(b) for $T_u = 90°C$ and $T_b = 20°C$ [and to a lesser extent in Fig. 7(b)] and the circulation are skewed towards the top for the same reason that they are skewed the other way in the N_2/water vapour mixture.

For the He/water vapour mixture, a comparison of Figs. 7(c) and 8(c) shows that, for given T_u, the liquid velocity increases as T_b decreases. In that case, a given temperature and the corresponding condensation of vapour occurs higher in the container, resulting in a greater difference between gravity and capillary forces; liquid velocities are therefore larger.

The TC model can be used to consider a temperature range which straddles a density minimum, but it is not then appropriate to compare those results with an SC model based on the usual linear density variation (i.e. constant $d\rho/dT$). In a subsequent paper, such results will be compared with an SC model based on a quadratic variation around the density minimum.

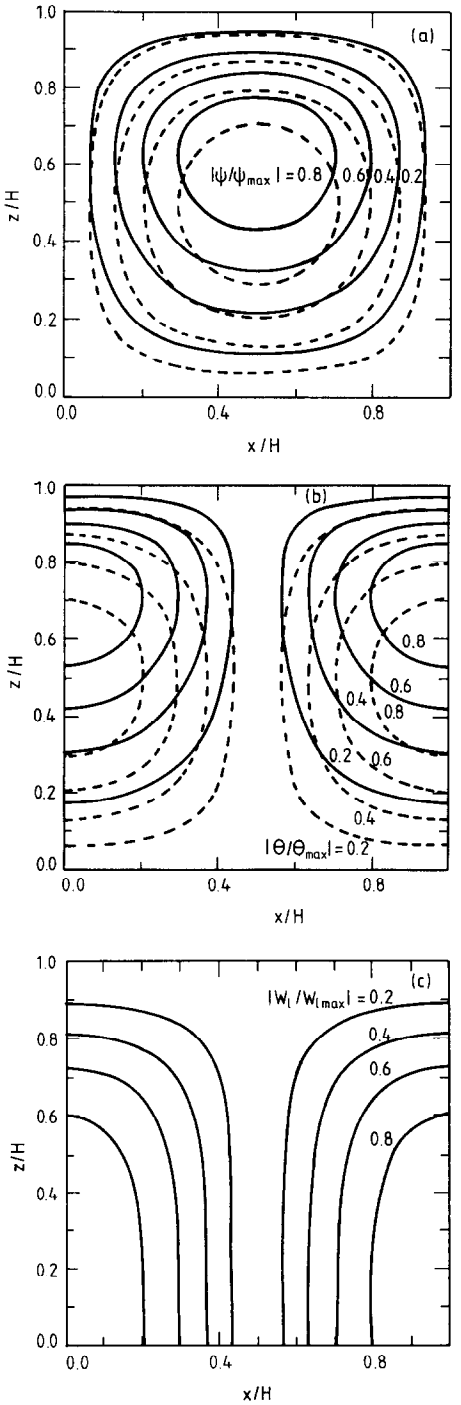

FIG. 8. (a) Stream function, (b) temperature perturbation, (c) (vertical) liquid velocity for onset mode of a helium/water vapour mixture when $T_u = 90°C$, $T_b = 20°C$ and $L/H = 1$. Solid lines correspond to the two-component model and dashed lines to the analogous single-component model. In (b) and (c), contour values on the left and right are of opposite sign.

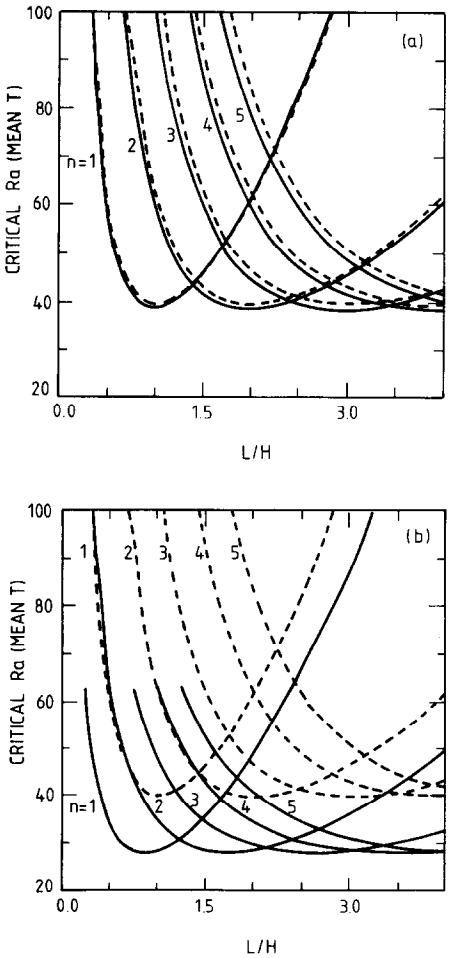

FIG. 9. Critical Rayleigh number evaluated at the mean temperature for nitrogen/water vapour as a function of L/H for the first 5 horizontal wave numbers when (a) $T_b = 90°C$, $T_u = 80°C$ and (b) $T_b = 90°C$, $T_u = 20°C$. Solid lines correspond to the two-component model and dashed lines to the analogous single-component model.

The TC and SC values of Ra_c, evaluated at the mean temperature for the N_2/water vapour mixture, are compared in Fig. 9 as functions of the aspect ratio L/H for the first 5 horizontal wave numbers. Results for the He/water vapour mixture are similar and are not shown. From Fig. 9(a), we see that, when $T_b = 90°C$ and $T_u = 80°C$, the SC and TC models predict the same number of convection modes (i.e. the same value of n minimises Ra_c at given L/H), except perhaps at values of L/H very near those at which the number of convection modes is changing. However, when $T_b = 90°C$ and $T_u = 20°C$ (i.e. ΔT is larger), the predicted number of SC and TC convection modes differs at a number of values of L/H. For example, when $L/H = 1.3$, the SC and TC models predict 1 and 2 circulation modes, respectively. Similarly, when $L/H = 2.3$, the corresponding number of modes is 2 and 3, respectively.

Acknowledgements—The author wishes to thank D. J. Close (CSIRO Division of Energy Technology) and W. J. Turner (CSIRO Division of Mineral Engineering) for helpful criticism and discussion of the manuscript.

REFERENCES

1. D. J. Close, Natural convection with coupled mass transfer in porous media, *Int. Comm. Heat Mass Transfer* **10,** 465–476 (1983).
2. D. J. Close and M. K. Peck, Some effects of natural convection in wet porous beds, Paper presented at the Third Australasian Conference on Heat and Mass Transfer. University of Melbourne, 13–15 May (1985).
3. P. Cheng, Heat transfer in geothermal systems, *Adv. Heat Transfer* **14,** 1–105 (1978).
4. J. G. Knudsen and D. L. Katz, *Fluid Dynamics and Heat Transfer*, p. 42. McGraw-Hill, New York (1958).
5. W. J. Minkowycz and E. M. Sparrow, Condensation heat transfer in the presence of noncondensables, interfacial tension, superheating, variable properties, and diffusion, *Int. J. Heat Mass Transfer* **9,** 1125–1144 (1966).
6. G. Schubert and J. M. Straus, Two-phase convection in a porous medium, *J. Geophys. Res.* **82,** 3411–3421 (1977).
7. E. Palm, J. E. Weber and O. Kvernvold, On steady convection in a porous medium, *J. Fluid Mech.* **54,** 153–161 (1972).
8. M. A. Combarnous and S. A. Bories, Hydrothermal convection in saturated porous media, *Adv. Hydrosci.* **10,** 231–307 (1975).
9. D. K. Edwards, V. E. Denny and A. F. Mills, *Transfer Processes*, p. 331. McGraw-Hill, New York (1976).
10. K. Wark, *Thermodynamics*, 2nd edn, p. 706. McGraw-Hill, New York (1971).

CONVECTION NATURELLE DES MELANGES GAZ-VAPEUR DANS UN MILIEU POREUX

Résumé—Un modèle à deux composants de la convection naturelle des mélanges gaz-vapeur est décrit en y introduisant la variation des propriétés du mélange en fonction de la température. L'attention est portée sur un lit fixe bidimensionnel avec des plans isothermes au-dessus et au-dessous et des parois latérales isolées ; on considère des mélanges azote-vapeur d'eau et hélium-vapeur d'eau. Quand la densité du mélange est une fonction monotone de la température et la différence de température est petite ($\sim 10°C$), les valeurs prédites du nombre de Rayleigh critique (Ra_c), les modes de convection, la distribution de vitesse et de température s'accordent bien (1–2% pour Ra_c) avec les valeurs correspondantes dérivées d'un modèle analogue à un seul composant basé sur les propriétés évaluées à la température moyenne ; on montre aussi la différence croissante entre ces valeurs quand la différence de température augmente.

NATÜRLICHE KONVEKTION VON GAS/DAMPFGEMISCHEN IN EINEM PORÖSEN MEDIUM

Zusammenfassung—Ein Zweikomponentenmodell der natürlichen Konvektion von Gas/Dampfgemischen wird beschrieben, in dem die Temperaturabhängigkeit der Gemisch-Stoffeigenschaften enthalten ist. Besondere Aufmerksamkeit wird einem zweidimensionalen Festbett mit einer isothermen Deck- und Bodenplatte und wärmegedämmten Seitenwänden gewidmet; die Gemische Stickstoff/Wasserdampf und Helium/Wasserdampf werden untersucht. Wenn die Gemischdichte eine monotone Funktion der Temperatur ist und eine geringe Temperaturdifferenz ($\cong 10$ K) vorliegt, stimmen die vorhergesagten kritischen Rayleigh-Zahlen (Ra_c), das Konvektionsbild, die Strömungs- und die Temperaturverteilung (1–2% in Ra_c) gut mit den dazugehörigen Werten überein, die aus einem analogen Einkomponentenmodell hergeleitet wurden, bei dem die Stoffwerte lediglich bei der mittleren Temperatur berechnet wurden; bei ansteigender Temperaturdifferenz werden die Abweichungen zwischen den genannten Werten ebenfalls größer.

ЕСТЕСТВЕННАЯ КОНВЕКЦИЯ ГАЗО–ПАРОВЫХ СМЕСЕЙ В ПОРИСТОЙ СРЕДЕ

Аннотация—Описывается двухкомпонентная модель естественной конвекции газо–паровых смесей, в которой учитывается температурная зависимости свойств смеси. Рассматривается двумерный плотный слой с изотермической верхней и нижней пластинами и изолированными боковыми стенками. Исследованы смеси азот–водяной пар и гелий–водяной пар. В случае, когда плотность смеси является монотонной функцией температуры и разность температур мала ($\approx 10°C$), рассчитанные значения критического числа Рэлея (Ra_c), режимы конвекции, распределения потока и температуры хорошо согласуются (1–2% Ra_c) с соответствующими значениями, полученными из аналогичной однокомпонентной модели, параметры которой оценены при средней температуре. Показано, что с ростом разности температур возрастает различие между значениями этих величин, полученными с помощью однокомпонентной и двухкомпонентной моделей.